Simulation of SVPWM Based FOC of CSI Fed Induction Motor Drive

Deepak Ronanki, Rajesh.K and Parthiban.P, *Member, IEEE*

***Abstract*— The application of current source inverters (CSI)in induction motor (IM) drives offers a number of advantages, including voltage boosting capability, natural shoot-through short-circuit protection and generation of sinusoidal voltages. In this paper, an attempt to model the CSI fed IM drive is presented. The mathematical model takes into account of the inverter, and induction motor dynamics and is established in the stationary reference frame. For controlling the drive speed, a direct field-oriented control (FOC) is proposed. To counter the effects of torque pulsations at very low speeds and the rotor resistance variation, a slip angle compensation loop is included in the control law formulation. Analytical expressions for CSI fed IM with Direct FOC are derived and validated using MATLAB/SIMULINK.**

***Index Terms*—CSI, Direct FOC, Induction Motor, MATLAB, SVPWM.**

I. Introduction

AMONG all types of machines the squirrel cage induction motors are most commonly used in the low and medium power (<160kW) variable-speed drives [1]. Squirrel cage induction motors are simple in construction, economical, rugged, reliable, and are available in a wide power range [1]. Besides traditional industrial drives, i.e. pumps, fans, cranes, automation drives, at present the induction motors are used in hybrid electric vehicles (HEV) and battery powered electric vehicle (BEV) providing high performance of torque control [2]. In the field of wind energy systems, for the last decade, the squirrel cage induction machines are increasingly employed in multi stage geared small wind generation systems (<100kW) with back-to-back converters connected to grid.

Generally, the two groups of power converter topologies can be applied to variable speed IM drives: VSI (voltage source inverter) and CSI (current source inverter). Nowadays, the current regulated PWM VSI for a high performance ac drive has been preferred to the CSI since the circuit cost is low, the control is simple, and the current loop has a wide bandwidth. However, it has drawbacks such as weakness to arm short failure and high dv/dt due to the pulse width modulated voltages of the inverter, and acoustic noise. The dv/dt may cause an insulation deterioration of the motor windings even though the acoustic noise can be eliminated by the high switching frequency (>1MHz). In addition, since the VSI does not keep a regeneration capability, the dynamic braking circuit has to added.

The application of high switching frequency (>20 kHz) silicon (Si) power transistors (IGBTs and RB-IGBTs) [3]-[5] and recently, the application of high switching frequency(>100kHz) silicon carbide (SiC) devices (SiCJFETs and SiC diodes) [6]-[7] has an enormous influence on applications of systems based on CSI and creates new possibilities. With the increase of switching frequency the volume of DC link inductors significantly decreases. Moreover the volume of the output filter capacitors decreases taking the fractional value of the VSI DC link capacitor. The SiC devices offer the possibility of a high blocking voltage and a low on-state resistance, which is the key parameter of the CSI.

CSI-fed induction motor drives have generally been used in high-horse power adjustable-speed applications. Many strategies have been proposed for controlling the motion of CSI-fed induction motor drives; to name a few, slip control, synchronous control, angle control, field-oriented control, and others. There are several requirements on designing a high-performance CSI-fed induction motor drive: the speed responses must be smooth without cogging or torque pulsations at low speeds; speed reversals are smooth under loading conditions; the drive system has symmetrical four quadrant operation; and the system is in constant full-torque operation below the rated speed and in constant horsepower operation at reduced flux above the rated speed. Among the many proposed control schemes, the field-oriented control has emerged as one of the most effective techniques in designing high-performance CSI-fed induction motor drives.

There are several modulating techniques applied for the CSI, including trapezoidal pulse width modulation (TPWM), selective harmonic elimination (SHE), and space vector modulation (SVM). Compared with TPWM and SHE, SVM provides more control flexibility and better dynamic performance.

This paper presents the mathematical model of IM, SVPWM, FOC, and CSI. All the above mentioned mathematical models are implemented in MATLAB/SIMULINK by using only basic Simulink blocks.

Deepak Ronanki is presently pursuing M.Tech in Power and Energy systems at National Institute of Technology Karnataka, Surathkal, Karnataka, India-575025 (email:deepuronnitk@gmail.com)

Rajesh.K is with the Department of Electrical Engineering, Vignan's LARA Institute of Technology and Sciences, Vadlamudi, Andhra Pradesh, India (e-mail: rajesh.kattiboina@gmail.com).

Parthiban.P are with the Department of Electrical Engineering, National Institute of Technology Karnataka, Surathkal -575025, India (e-mail: parthdee@nitk.ac.in).

978-1-4673-0455-9/12/$31.00 ©2012 IEEE

II. Description and Modeling of CSI fed Induction Motor Drive

Fig.1. shows the main circuit configuration of the six-switch three-phase CSI. This inverter comprises a constant DC power supply, an inverter section to convert the DC power to the variable-voltage frequency AC power and an induction motor at the load side. Moreover, three capacitors are connected to the AC terminals to absorb the over voltages which occur when the current is cutoff. The overvoltage absorption capacitors which are connected to the AC terminals function as a filter, therefore the output current has a sinusoidal waveform.

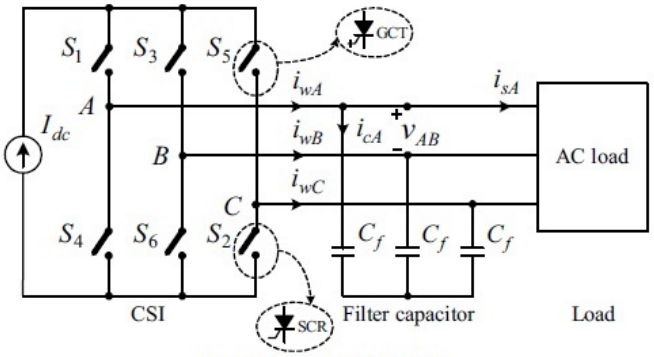

Fig. 1. A Generalized six-switch three-phase CSI

A. Mathematical model of Induction Motor

The model of the induction motor consists of three-phase to two-phase transformation equations, electro-mechanical equations and load dynamic equations. Consider that three phase sinusoidal currents are impressed in the three phase stator windings, which are given as

$$i_A = \mathrm{I_m}\sin(\omega t) \tag{1}$$

$$i_B = \mathrm{I_m}\sin(\omega t - \frac{2\pi}{3}) \tag{2}$$

$$i_C = \mathrm{I_m}\sin(\omega t + \frac{2\pi}{3}) \tag{3}$$

The three-phase current source are transform into two phase i.e. abc to d-q transformation. The current equations for phase transformation as follows:

$$\begin{pmatrix} i_d \\ i_q \end{pmatrix} = \begin{pmatrix} \cos(\omega t) & \cos(\omega t - \frac{2\pi}{3}) & \cos(\omega t + \frac{2\pi}{3}) \\ \sin(\omega t) & \sin(\omega t - \frac{2\pi}{3}) & sin(\omega t - \frac{2\pi}{3}) \end{pmatrix} \begin{pmatrix} i_A \\ i_B \\ i_C \end{pmatrix} \tag{4}$$

$$\frac{d\psi_{dr}}{dt} = \frac{L_m}{\tau_r} i_{ds} - \omega_r \psi_{qr} - \frac{1}{\tau_r}\psi_{dr} \tag{5}$$

$$\frac{d\psi_{qr}}{dt} = \frac{L_m}{\tau_r} i_{qs} - \omega_r \psi_{dr} - \frac{1}{\tau_r}\psi_{qr} \tag{6}$$

where $\tau_r = \frac{L_r}{R_r}$ is the rotor circuit time constant. Equations (5) and (6) give rotor fluxes as functions of stator currents and speed. Therefore, knowing these signals, the fluxes and corresponding unit vector signals can be estimated. The electromechanical block configuration is based on the following equations. With the rotor voltage vector normally assumed zero, the torque equation in excitation reference is expressed as

$$T = \frac{3P}{4}(\frac{L_m}{L_r})(\psi_{dr} i_{qs} - \psi_{qr} i_{ds}) \tag{7}$$

The load dynamics block is based on below equation

$$\frac{d\omega_m}{dt} = -\frac{B}{J_m}\omega_m + \frac{T - T_L}{J_m + J_L} \tag{8}$$

From equation (9), the slip frequency ω_r can be calculated and fed back into the electromechanical block

$$\omega_r = \omega - \frac{P}{2}\omega_m \tag{9}$$

where Ψ_{dr}& Ψ_{qr} are d, q axis fluxes linkages; i_{ds}& i_{qs} d, q-axes currents; Lm is mutual inductance between the phases; $L_r$is rotor inductance; P is no of poles; T_L is load torque; $\acute{\omega}_m$ is mechanical speed of the motor; J_m is moment of inertia of motor; J_L is moment of inertia of load.

B. Modeling of current source inverter

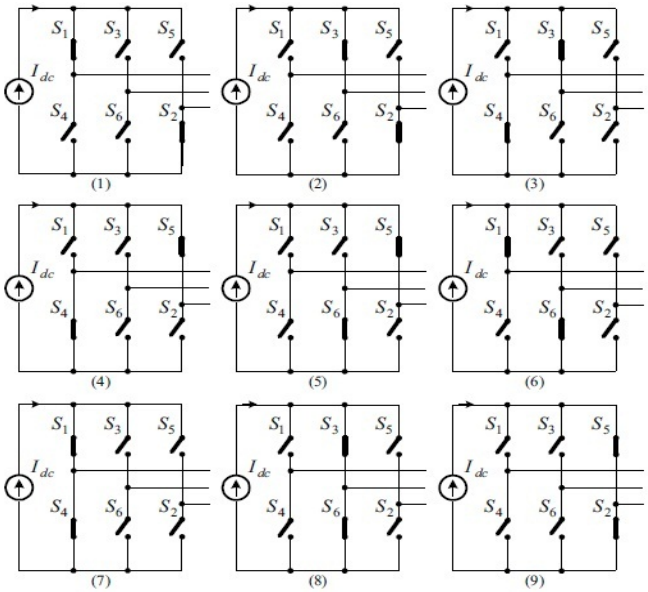

Fig. 2. Switching States for a Current Source Inverter

The switching pattern design for the CSI should generally satisfy two conditions: 1) DC current I_{dc} should be continuous, and 2) the inverter PWM current i_A, i_B, i_C should be defined. The two conditions can be translated into a switching constraint: At any instant of time (excluding commutation intervals), there are only two sets of series connected switches

conducting, i.e., one set in the top half of the bridge such as S_1 in Fig.1 and the other in the bottom half of the bridge such as S_2 . The switching function for switch S_m is defined as

$$S_m = \begin{cases} 0 \ S_m \text{ open} \\ 1 \ S_m \text{ closed} \end{cases} \quad m = 0,...6 \tag{10}$$

The switching constraint be satisfied if following equations are hold good

$$\begin{cases} S_1 + S_3 + S_5 = 1 \\ S_4 + S_6 + S_2 = 1 \end{cases} \tag{11}$$

There are nine out of 32 switching states developed from equation11. To generate a given set of ac line current waveforms, the inverter must move from one state to another. Thus, the resulting line currents consist of discrete values of current, which are I_{dc}, 0, I_{dc}. The selection of the states in order to generate the given waveforms is done by the modulating technique that should ensure the use of only the valid states 9. These valid 9 states are shown in theFig.2. The CSI output three-phase currents i_A, i_B and i_C are the functions of the DC-link current I_{dc} and the switching functions g= [S_1, S_2, S_3, S_4, S_5, S_6] as follows:

$$\begin{cases} i_A = (S_1 - S_4) I_{dc} \\ i_A = (S_3 - S_6) I_{dc} \\ i_A = (S_5 - S_2) I_{dc} \end{cases} \tag{12}$$

From equations (12) modeling of the CSI was built in MATLAB/SIMULINK.

III. Direct Field Orientation Control Of Induction Motor Drive

The essence of the FOC is the decoupled control of the rotor flux Ψ_r and electromagnetic torque T_e these two variables are controlled separately.

The induction motor is fed by a current-controlled space vector modulated inverter. The motor speed ώ is compared to the reference ώ* and the error is processed by the speed controller to produce a torque command T^*_e. The block diagram given in fig.3 shows a variable speed induction motor drive using field-oriented control.

The stator quadrature-axis current reference i^*_{qs} is calculated from torque reference T_e^* as given in (13)

$$i_q^* = \frac{2}{3}\frac{2}{P}\frac{L_m}{L_r}\frac{T_e^*}{\psi_r} \tag{13}$$

where L_r is the rotor resistance, L_m is the mutual inductance and Ψ_r is the estimated rotor flux linkage given by (14)

$$\psi_r = \frac{L_m i_{ds}}{1 + \tau_s} \tag{14}$$

where $\tau_r = \frac{L_s}{R_s}$ is the rotor constant. The stator direct-axis current reference i^*_{ds} is obtained from rotor flux reference input Ψr^* as follows

$$i_{ds}^* = \frac{\psi_r^*}{L_m} \tag{15}$$

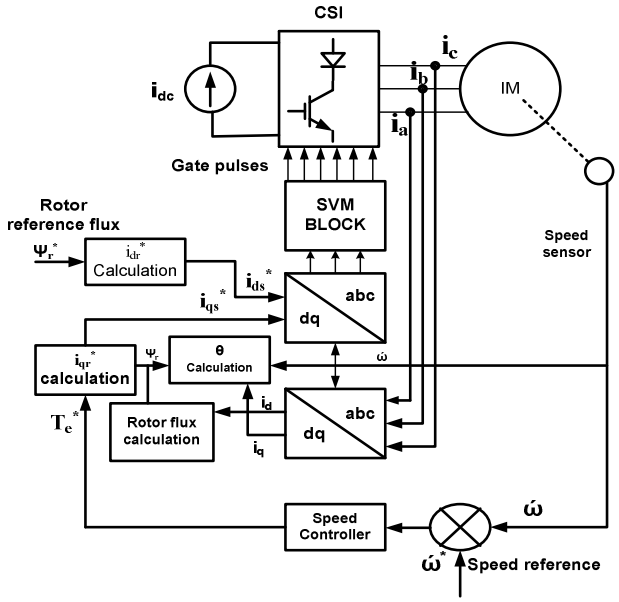

Fig. 3. Block Diagram of SVM based FOC of CSI fed IM drive

The rotor flux position θ_e required for coordinate transformation is generated from the rotor speed $\acute{\omega}_m$ and $\acute{\omega}_r$

$$\theta_e = \int (\omega_m + \omega_r) \tag{16}$$

The slip frequency is calculated from the stator reference current i_{qs} and the motor parameters in (17)

$$\omega_r = \frac{L_m R_r}{\psi_r L_r} i_{qs}^* \tag{17}$$

The i^*_{qs} and i^*_{ds} current references are converted into phase current references i^*_A, i^*_B and i^*_C then given as input to the SVM block.

IV. Modeling Of Space Vector Pulse Width Modulation

A. Space Current Vectors

A space current vector in complex notation is given by

$$I_k = \frac{2}{3}(i_A + \vec{a} i_B + \overrightarrow{a^2} i_c) \tag{18}$$

where $\vec{a} = e^{j\frac{2\pi}{3}}$ The PWM CSI uses six unidirectional switches to connect the dc current source to the load. Two switches in two different legs, one in the upper switch bridge (S_1; S_3; S_5) and the other in the lower switch bridge in Fig.1 are allowed to conduct at any instant. It is noted that there

should always exist a current path in the CSI. If not, a high voltage at open terminal is induced so that the switch might be destroyed. The CSI can generate only six effective space vectors and three zero vectors. The zero vectors mean that both the upper and lower switches in the same arm are turn-on state simultaneously. The space current vectors are illustrated in Fig.4.

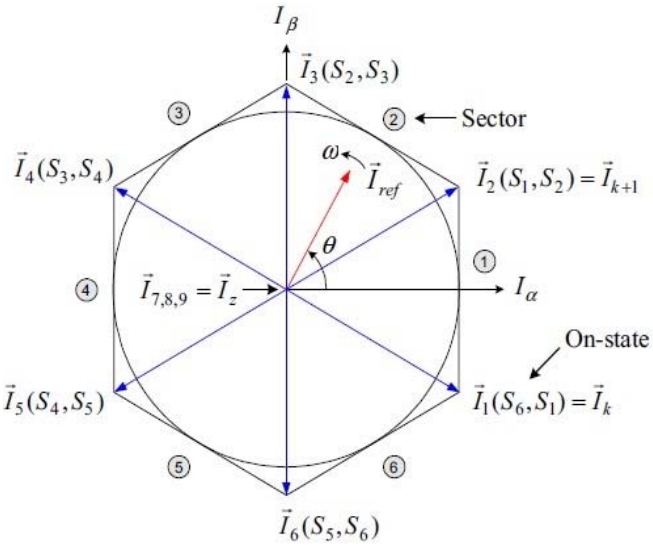

Fig. 4. Space Vector Diagram for Current Source Inverter

The main function of SVM block is to generate six switching pulses to six switches of the CSI inverter so that the desired phase currents are obtained. The input to the SVM block is the three reference currents i^*_A, i^*_B and i^*_C and the DC link current I_{dc}.

$$\begin{pmatrix} i_d \\ i_q \end{pmatrix} = \frac{2}{3}\begin{pmatrix} 1 & \frac{-1}{2} & \frac{-1}{2} \\ 0 & \frac{\sqrt{3}}{2} & \frac{-\sqrt{3}}{2} \end{pmatrix}\begin{pmatrix} i_A \\ i_B \\ i_C \end{pmatrix} \tag{19}$$

This transformation can be used with three phase currents associated with three-phase six-switch current source inverters. From which we can calculate i_{ref} , θ as

$$i_{ref} = \sqrt{i_d^2 + i_q^2} \tag{20}$$

$$\theta = \arctan(\frac{i_q}{i_d}) \tag{21}$$

B. Dwell Time Calculations

The dwell time calculation is based on ampere-second balancing principle, i.e, the product of the current reference vector I_{ref} and sampling period T_s equals the sum of the current vectors multiplied by the time interval of chosen space vectors. Assuming that the sampling period T_s is sufficiently small, the current reference vector I_{ref} can be considered constant during Ts. So can be considered constant during T_s. So I_{ref} can be approximated by two adjacent active vectors I_k, $I_{(k+1)}$ and a zero vector I_z. To ensure that the generated current in one sampling period T_s made up of the currents provided by the vectors I_k, $I_{(k+1)}$ and I_z used during times T_1, T_2 and T_z is on average equal to the current reference vector I_{ref} the dwell time can be obtained by

$$T_1 = m_a T_s \sin(\frac{\pi}{6} - \theta + (n-1)\frac{\pi}{6}) \tag{22}$$

$$T_2 = m_a T_s \sin(\frac{\pi}{6} - \theta - (n-1)\frac{\pi}{6}) \tag{23}$$

$$T_z = T_s - T_1 - T_2 \tag{24}$$

where $m_a = \frac{I_{ref}}{I_{dc}} = \frac{I_1}{I_{dc}}$ is modulation index, I_1 is the peak value of the fundamental frequency component of (i_A, i_B and i_C) and n is sector number.

TABLE I
SWITCHING STATES AND SPACE VECTORS

Type	Switching State	On-state switch	Inverter pwm current			Space vector
			i_A	i_B	i_C	
ZERO STATES	[14]	S_1,S_4	0	0	0	I_0
	[36]	S_3,S_6	0	0	0	I_0
	[52]	S_2,S_5	0	0	0	I_0
ACTIVE STATES	[61]	S_6,S_1	I_{dc}	$-I_{dc}$	0	I_1
	[12]	S_1,S_2	I_{dc}	0	$-I_{dc}$	I_2
	[23]	S_2,S_3	0	I_{dc}	$-I_{dc}$	I_3
	[34]	S_3,S_4	$-I_{dc}$	I_{dc}	0	I_4
	[45]	S_4,S_5	$-I_{dc}$	0	I_{dc}	I_5
	[54]	S_5,S_6	0	$-I_{dc}$	I_{dc}	I_6

C. Switching sequence

The PWM switching pattern for the CSI must satisfy a constraint, i.e, only two switches in the inverter conduct at any time instant, one in the top half of the CSI bridge and the other in the bottom half. Under this constraint, the three phase inverter has a total of nine switching states as listed in Table I. These switching states can be classified as zero switching states and active switching states. There are three zero switching states (14), (36), and (52). The zero state (14) signifies that switches S_1 and S_4 in inverter phase leg A conduct simultaneously and the other four switches in the inverter are OFF. The DC current source I_{dc} is by passed, leading to $i_A = i_B = i_C = 0$. This operating mode is often referred to as by-pass operation. There exist six active switching states. State [12] indicates that switch S_1 in leg A and S_2 in leg C are ON. The DC current I_{dc} flows through S_1, the load, S_2, and then back to the DC source, resulting in $i_A = I_{dc}$ and $i_C = I_{dc}$. The definition of other five active states is given in the Table I.

TABLE II
COMPARISON OF CSI MODULATION TECHNIQUES

Item	SVM	TPWM	SHE
DC current utilization	0.707	0.74	0.73-0.78
Dynamic performance	High	Medium	Low
Digital implementation	Real time	Real time or Look-up table	Look-up table
Harmonic performance	Adequate	Good	Best
DC current bypass operation	Yes	No	Optional

V. SIMULATION RESULTS AND DISCUSSIONS

The comparison of CSI modulation techniques is shown in the Table II. The Direct FOC scheme for CSI fed Induction Motor drive has been simulated in MATLAB/SIMULINK. The simulation parameters have been given in appendix. The simulated waveforms of DC current, motor current, reference torque, estimated torque, reference speed and actual speed are shown in Figs.5-9. The simulation is carried out for two different cases. In case-I with Different Reference Speeds at constant load torque and case-II with Different Load Torques at constant reference speed.

Case-I: In this section the behaviour of Induction motor at two reference speeds are observed. When I_{dc} = 20A, K_p=3, and K_i=0.000004. Different reference speeds are applied at 0.2sec. for this case the simulated waveforms are shown in figs.5-7. The Fig.5 shows the waveform of inverter input DC current and motor input i.e. stator current of phase A. The Fig.6 shows the waveform of the Reference Speed and Actual Speed of the motor when the ω_r =130 rad/sec. The Fig.7 shows the waveform of the Reference Speed and Actual Speed of the motor when the ω_r =110 rad/sec.

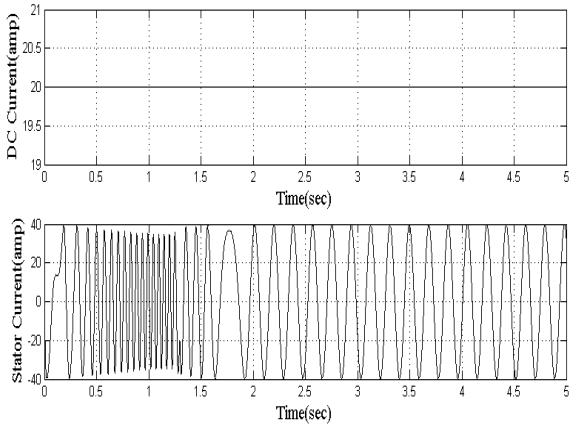

Fig. 5. The waveforms of Inverter Input (DC current) and Output (Stator current)

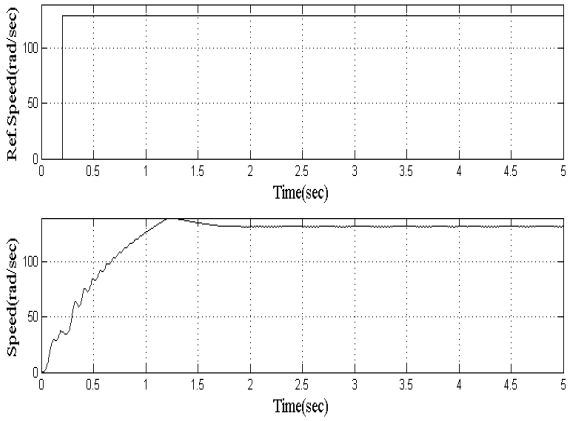

Fig. 6. The waveform of the Reference Speed and Actual Speed of the motor when the ω_r=130 rad/sec

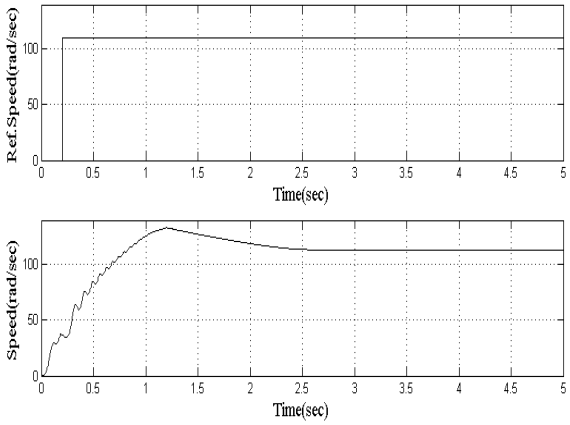

Fig. 7. The waveform of the Reference Speed and Actual Speed of the motor when the ω_r =110 rad/sec

Case-II: In this section the behaviour of Induction motor at two different load torques are observed. When I_{dc} = 20A, K_p=3, and K_i=0.000004. The two different load torques are applied at 1.2sec. The Fig.8 shows the wave form of the Reference Torque and Actual Torque of motor when the T_L is at 10N-m. The Fig.9 shows the wave forms of the Reference Torque and Actual Torque of motor when the T_L is at 5N-m.

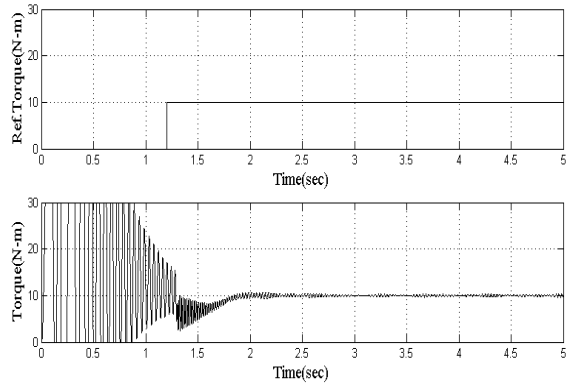

Fig. 8. The waveforms of the Reference Torque and Actual Torque of motor when the T_L is at 10N-m

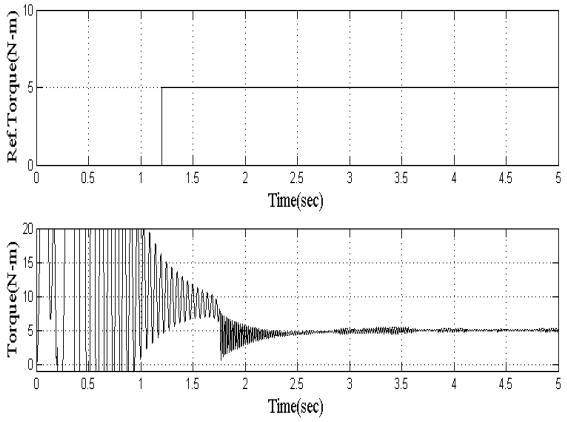

Fig. 9. The waveforms of the Reference Torque and Actual Torque of motor when the T_L is at 5N-m

VI. APPENDIX

Parameters used in the simulation are Rated power (P)=7.5kW, V=220V, f=50Hz, $\acute{\omega}_r$=1440rpm. The Induction motor parameters are Stator resistance (R_s)=0.294Ω, Stator inductance (L_s)=0.0425H, Stator leakage reactance (X_{ls})= 0.524Ω, Rotor resistance (R_r)=0.156Ω, Rotor inductance (L_r)=0.0418H, Rotor leakage inductance referred to stator (X_{lr})= 0.0418H, J_m=0.4kg-m^2, B=0.062, P=4.

VII. CONCLUSIONS

This paper presents advantages of CSI compared to VSI due to advancements in power semiconductor devices used in CSI which is best suited for variable speed drive applications. In this paper, the mathematical model of CSI, Induction Motor, SVPWM and control of IM with direct FOC has been explained in detail. Analytical expressions for CSI fed Induction Motor with Direct FOC are derived and validated using MATLAB/SIMULINK by using only basic Simulink blocks. The switching time calculations and switching states are discussed in detail. The proposed scheme control of CSI fed Induction motor drive has good dynamic performance.

VIII. REFERENCES

[1] Bimal K. Bose: Power Electronics And Motor Drives: Advances andTrends, Elsevier, 2006.

[2] Adamowicz, M.; Morawiec, M.; , "Advances in CSI-fed induction motor drives," *Compatibility and Power Electronics (CPE), 2011 7th International Conference-Workshop* , vol., no., pp.276-282, 1-3 June 20

[3] Yun Wei Li, Manish Pande, Navid Reza Zargari, Bin Wu; "An InputPower Factor Control Strategy for High-Power Current-SourceInduction Motor Drive With Active Front-End,." *IEEE Tran. On Powerelectronics* , Vol.25, No.2, pp.352-359, February 2010.

[4] Eduardo P. Wiechmann, Pablo Aqueveque, Rolando Burgos, Jos Rodrguez;"On the Efficiency of Voltage Source and Current Source Invertersfor High-Power Drives,." *IEEE Tran. On Industrial electronics* , Vol.55, No.4, pp.1771-1820, April 2008.

[5] Fuchs F., Kloenne A; "DC link and Dynamic Performance Features of PWM IGBT Current Source Converter Induction Machine Drives with Respect to Industrial Requirements,." *Proc. IEEE Conference IPEMC* 2004 , Vol.3, 14-16.

[6] Colli V.D., Cancelliere P., Marignetti F., Di Stefano R; "Voltage controlof current source inverters,." *IEEE Tran. On Energy Conversion*, Vol.21, No.2, pp.451-458, June 2006.

[7] T. Friedli, S. Round, D. Hassler, J. W. Kolar,; "Design and Performanceof a 200-kHz All-SiC JFET Current DC-Link Back-to-Back Converter,."*IEEE Tran. On Industry Applications*, Vol.45, No.5, pp.1868-1878, Sep/Oct 2009

[8] Parthiban, P.; Agarwal, P.; Srivastava, S.P.; , "A Simplified Space-Vector Modulated Control Scheme for CSI fed IM drive," *Power Electronics, Drives and Energy Systems, 2006. PEDES '06. International Conference on* , vol., no., pp.1-6, 12-15 Dec. 2006

[9] Cass C. J., Wang Y., Burgos R., Chow T. P., Wang F., Boroyevich D;"Evaluation of SiC JFETs for a Three-Phase Current-Source Rectifierwith High Switching Frequency,." *Proc. Twenty Second AnnualIEEE Applied Power Electronics Conference APEC 2007*, pp.345-351.

[10] M. Salo and H. Tuusa,; "A vector-controlled PWM currentsource inverter fed induction motor drive with a new stator current control method,." *IEEE Tran. On Industrial electronics* , Vol.52, No.2, pp.523-531, April 2005.

[11] N. R. Zargari, S. C. Rizzo,; "A New Current-Source Converter Usinga Symmetric Gate-Commutated Thyristor (SGCT),." *IEEE Tran. On Industry applications*,Vol.37, No.23, pp.896-903, April 2001.

[12] A. M. Qiu, Y.W. Li, N. Zargari, Y. Liu;"High Performance Current Source Inverter Fed Induction Motor Drive with Minimal Harmonic Distortion,." IEEE-PESC 2007, pp.79-85, June 2007.

[13] Chang-Huan Liu, Chen-Chain Hwu, and Ying-Fang Feng; "Modelling and Implementation of a Microprocessor-Based CSI-Fed Induction Motor Drive Using Field-Oriented Control." IEEE Tran. on IPCSD, Vol.39, No 07 , Dec 1988

[14] Masahiro Kaimoto, Makoto Hashii, Takao Yanase, and TakayoshiNakano; "Performance Improvement of Current Source Inverter-Fed Induction Motor Drives,." IEEE Paper in IPCSD , Vol.29, No.14, April 1982.

[15] Bin Wu:, High-Power Converters And AC Drives, A John Wiley and sons, Inc, Publication